Peer-reviewed version available at Coatings 2018, 8, 184; doi:10.3390/coatings8050184

Article

Hydrophilic self-replenishing coatings with long-term water stability for anti-fouling applications

Isabel Jiménez-Pardo [1], Leendert G.J. van der Ven [1], Rolf A.T.M. van Benthem [1,2], Gijsbertus de With [1,*], A. Catarina C. Esteves [1,*]

[1] Laboratory of Physical Chemistry, Department of Chemical Engineering and Chemistry, Eindhoven University of Technology, Eindhoven, the Netherlands;
[2] DSM Materials Science Center BV Netherlands, Geleen, the Netherlands.
* Correspondence: a.c.c.esteves@tue.nl; Tel.: +31 40 247 3034; g.dewith@tue.nl; Tel.: +31 40 247 4947

Abstract: Hydrophilic coatings have recently emerged as a new approach to avoid the adhesion of (bio)organisms on surfaces immersed in water. In these coatings the hydrophilic character is crucial for the anti-fouling (AF) performance. However, this property can be rapidly lost due to the inevitable damages which occur at the surface, reducing the long-term effectiveness of the AF functionality. We report hydrophilic polycarbonate-mPEG polyurethane coatings with tunable hydrophilic properties as well as an excellent and long-term stability in water. The coatings exhibit low protein adhesion values and are able to self-replenish their hydrophilicity after damage, due to the existence of a reservoir of hydrophilic dangling chains incorporated in the bulk. The combination of low T_g and sufficient mobility of the mPEG dangling chains (enabled by chains with higher molecular weight) proved to be crucial to ensure autonomous surface hydrophilicity recovery when the coatings were immersed in water. This coatings and design approach offer new possibilities towards high performance AF coatings with an extended service life-time which can be used in several major applications areas, such as marine and biomedical coatings, with major economic and environmental benefits.

Keywords: Self-replenishing; Anti-fouling; Hydrophilic Coatings; Polycarbonate; mPEG; Dangling chains.

1. Introduction

Coatings which are immersed or permanently in contact with water will inevitably accumulate organisms on their surface, *i.e.* bio-fouling will take place. This phenomenom is of major relevance in many application fields. In marine coatings, for example, the accumulation of fouling leads to an increased drag resistance and higher fuel consumption.[1] Furthermore, it requires frequent maintenance and dry-dock repair which have a highly negative environmental and economic impact.[2] Another example is in the medical field, where coatings are applied on medical devices, such as catheters and contact lenses to provide a certain lubricious property. Accumulation of foulants such as blood cells, components from body fluids or even bacteria and viruses would increase the friction resulting in wounds due to the rupture of cells and also induce infections.[3-4]

Several anti-fouling (AF) strategies have been reported for polymer coatings in which the characteristics of the top surface, *i.e.* chemical composition and topography, are critical for the effectiveness and long time performance of this surface functionality, as discussed in several literature reviews available.[5-9] More recently, hydrophilic high surface energy coatings emerged as an interesting option to prevent the adhesion of foulants, most of them making use of the well-known anti-fouling character of polyethylene glycol (PEG)-based derivatives.[10-14] Although the working principle of this type of coatings is still unclear and several mechanisms have been proposed by different authors, [8,15-16] it is widely assumed that the use of hydrophilic polymeric surfaces allows the formation of a hydration layer by means of hydrogen bonding between the water molecules and

the hydrophilic polymer, which reduces the probability of proteins to adhere to the surface, thus reducing the initial attachment and subsequent accumulation of foulants. However, once the coating is damaged and the surface characteristics (in this case the hydrophilicity) are lost upon wear, degradation or attachment of the first biorganisms, the AF properties are no longer effective and the wet surfaces will become rapidly fouled. Introducing a self-repairing mechanism, which can intrinsically replenish the damaged surface with new hydrophilic AF chemical moieties, would allow a high AF performance level throughout the life-time of the coatings, with major economic and environmental benefits.

As previously demonstrated for analogous hydrophobic coatings, [17-19] an intrinsic and spontaneous self-replenishing mechanism can be incorporated in coatings by fulfilling some design requirements. The coating should contain: *i)* a reservoir of hydrophilic dangling chains chemically bonded to the bulk network; *ii)* these dangling chains should be sufficiently mobile, *e.g.* typically governed by a low T_g of the polymer components, to reorient upon creation of new interfaces and *iii)* a proper hydrophilic-hydrophobic balance between all the coating components (*i.e.* dangling chains and network polymer precursors), which will provide the driving force for the reorientation of the dangling chains towards the air-coating, or in this case, water-coating, interface once damage occurs.

Up to date most of the self-replenishing systems found in literature are hydrophobic while the development of self-healing hydrophilic coatings is still scarcely addressed.[20-23] In one of the few examples Minko *et al*. settled guidelines towards the design of materials with long-lasting hydrophilicity and anti-fouling properties. The hydrophilicity and AF properties of PEG 2D surface-grafted and 3D-network grafted films, possessing PEG chains in the surface and inside the network film, were studied and compared. For the measuring time of four weeks used, the 3D-grafting structures demonstrated much higher hydrophilicity stability and fouling resistant properties than the 2D films due to the spontaneous rearrangement of the chains stored inside the film.[22] In a more recent publication self-assembled microgel spheres with grafted hydrophilic chains were synthesized. The films presented oil-repellent and AF properties, and were able to self-repair after induced damage. Also in this case, the self-healing function was attributed to the 3D structure combined with the presence of a reservoir of hydrophilic chains. [23]

It should also be noted that, while for some specific applications a easily degradable polymer coating may be required (e.g. for short-term medical implants) for many others, the overall long term stability of the hydrophilic self-healing coatings when immersed in water and the absence of leachable materials (i.e. resulting from bulk or network degradation) are essential, e.g. in the marine field and especially on medical devices in contact with the human skin or body-fluids.

The current study focuses on developing hydrophilic self-replenishing coatings, targeting application areas such as marine or medical AF coatings. To this purpose we designed three component polyurethane-based networks, with a mixture of tri-branched and linear poly(1,3-propylene)carbonates (PC) as polymeric matrix, a triisocyanate (tHDI) as crosslinker and PEG moieties as hydrophilic dangling chains, which preferentially orient towards the water-coating interfaces providing AF properties.

The preparation of the AF hydrophilic networks and their characterization by FTIR, DSC, static and dynamic contact angle and water uptake measurements is presented. The long-term stability and appearance of the coatings in water is addressed and the anti-fouling potential is discussed, based on preliminary protein adsorption measurements.

The design of the coatings was directed to provide self-replenishing characteristics, *i.e.* to recover the surface hydrophilicity and related functionalities. The recoverability of the surface properties in water is demonstrated by dynamic contact angle measurements, before and after, controlled damage which was intentionally induced at the coatings surface.

2. Materials and Methods

1,3-propanediol, ethyl chloroformate, triethylamine (TEA), trifluoroacetic acid (TFA, 99% for HPLC), pyridine, poly(ethylene glycol) methyl ether with average M_n of 550 and 2000 g·mol^{-1} (mPEG550 and mPEG2000, respectively), and Fibrinogen (FB, ~340 kDa) were purchased from Sigma-

Aldrich. Poly(ethylene glycol) methyl ether average M_n 1000 g·mol^{-1} (mPEG1000) was purchased from TCI chemicals. A polyisocyanate crosslinker, Desmodur N3600 containing primarily a trimer of hexamethylenediisocianate (further noted as tHDI, hydroxyl group functionality 2.8) was kindly supplied by Perstorp. Aluminium oxide 90 active neutral (activity stage I) used for column chromatography was purchased from Merck. The Phosphate Buffer Saline (PBS) solution 1X pH 7.4 was purchased from Thermo Fischer Scientific. Organic solvents were purchased from Biosolve. Trimethylolpropane (TMP) was purchased from Merck and dried at 45 °C during 3 hours before use. All the other chemicals were used as received.

Polymers characterization. ^{1}H-NMR and ^{13}C-NMR spectra were recorded on a Varian and Bruker spectrometer, operating at 400/100 MHz or 500/125 MHz (Varian Inova). $CDCl_3$ with TMS as an internal standard was used as the solvent. Fourier Transform-Infrared (FT-IR) Attenuated Total Reflectance (ATR) Spectroscopy was performed on a Varian 3100 FT-IR spectrometer with DTGS detector, collecting an average of 50 scans in the frequency range from 600 to 4000 cm^{-1}. GPC measurements were performed on a Waters Alliance system GPC equipped with a Waters model 1515 pump and a model 2414 refractive index detector. A set of two columns (SDV 500 Å, PSS, 30 cm, 40 °C and a guard column (SDV 5 µm, PSS) was used and THF was selected as eluent with a flow of 1 mL min^{-1}. The system was calibrated using narrow molecular mass polystyrene standards ranging from 139 to 39 000 g mol^{-1}. The polymers were dissolved in THF at a concentration of 1 mg mL^{-1}. Matrix-assisted laser desorption/ionization time-of-flight mass spectrometry (MALDI-ToF MS) measurements were performed on a Voyager-DE Pro instrument (Perspective Biosystems, Framingham, MA). The polymers were dissolved in THF at a concentration of 5 mg mL^{-1}. Potassium trifluoroacetate (KTFA) was used as the ionizing agent and trans-2-[3-(4-tert-butylphenyl)-2-methyl-2-porpenylidene] malononitrile (DCTB) was used as matrix. The isotopic distributions were analyzed using DataExplorer Advanced Biosystems.

The thermal properties of the coatings (5 to 10 mg samples) were studied by ThermoGravimetric Analysis (TGA) on a TA Q500 equipment, heating from 25 to 600 °C at 10 °C/min under a nitrogen flow. DSC measurements were performed on a TA DSC Q100. Samples (6-8 mg) were measured with a heating-cooling-heating cycle that runs from –80 °C until 80 °C at 10 °C/min under a nitrogen flow. The second heating run was selected for the analyses of the results. The coating thicknesses were measured on a Veeco Dektak 150 profilometer.

Determination of extractables. The amount of non-reacted or non-network incorporated species was extracted from coatings by immersing a known amount of coating detached from the substrate (typically 50-100 mg) in water and acetone. After 24 hours immersion the coatings were dried overnight in vacuum at 45 °C. The weight loss (%) was calculated from the mass of coating after extraction divided by the mass coating before extraction x 100. Each coating was measured in triplicate. Water and acetone liquid extracts were evaporated at room temperature and afterwards vacuum dried at 45 °C overnight to recover and analyze the extracted solid residues by ^{1}H-NMR.

Contact Angle. Static and dynamic contact angle measurements were performed on a DataPhysics contact angle system (OCA30) by using distilled water as a probe liquid. For static measurements water droplets of 8 µl were deposited on the surface. For dynamic measurements the advancing water contact angle (CA_{Adv}) was measured with the ARCA software tool in the following way: a 2 µl droplet was first placed on the surface. Water was then injected into the droplet up to 8 µl at 0.5 µl/s. After a waiting period of 2 seconds water was retracted from the droplet by using the same settings as for the water injection. Each coating was measured in triplicate. All measurements were done in coatings previously soaked in water to minimize the water absorption effect.

Water uptake. The water uptake (%) was calculated from the following equation: $Wt–W_0/W_0*100$, where W_t is the weight of the swollen coating at a specific time and W_0 the initial weight of the dry coating. Each coating was measured in triplicate. Typically, ≈ 50-100 mg of the free standing film coatings were immersed in demineralized water. The amount of absorbed water was measured gravimetrically at several immersion times. The water absorption experiments allowed to determine the percentage of water uptake after 24 hours as well as the degradation of the coatings which was evaluated over one year.

Coating damage. Controlled damage was induced on dry coatings by using a set-up previously described for self-replenishing studies on hydrophobic coatings.[18] A piece of 1200/4000 grit silicon carbide sand paper (2×2.4 cm) was glued to a metal disk which was loaded with additional metal rings with a final mass of 30.9 g, resulting in a constant pressure on the abrasion area of about 4300 Pa. To perform the abrasion test, the sandpaper (with the metal disks on top of it) was applied on the coatings surface and moved manually along the parallel direction (back and forth). The extent of damage was detected by measuring the thickness (Veeco Dektak 150 profilometer) and the surface wettability (CA_{Adv}) before and after damage. The sand paper was replaced every 50 cycles to avoid transfer of debris and contamination. The surface hydrophilicity recovery was quantified by calculating the Self-Replenishing Efficiency (SRE), where $CA_{initial}$ is the water CA of the coatings before damage and CA_{final} is the water CA measured after damage and a specific time of self-replenishing.

$$\mathrm{SRE}\ (\%) = 100 - \left[\frac{\mathrm{CA_{final}} - \mathrm{CA_{initial}}}{\mathrm{CA_{initial}}} \times 100\right]$$

Protein adsorption. Coatings applied on glass substrates (20 mm x 20 mm) were first washed with acetone (5 x 1 ml) and extracted overnight with 25 ml of water to get rid of all non-reacted or non-network incorporated components (extractables) that could interfere in the measurement. The extracted coatings were dried in vacuum at 45 °C overnight. The dried coatings were rehydrated by immersing them in 5 ml of PBS solution for 1 hour. Next, the PBS soaked coatings were incubated for 24 hours with 700 µl of 1 $mg{\cdot}ml^{-1}$ FB protein solution in PBS, ensuring that the full coating surface was covered by the protein containing solution. Afterwards the coatings were washed (with 2 x 450 µl of PBS) to remove the non-adsorbed proteins. Following procedures previously reported in literature,[23-24] the amount of adsorbed proteins was determined in an indirect way by measuring the non-adsorbed proteins and subtracting this value from the initial known protein feed. For the quantification of the protein in the PBS solutions, the characteristic absorbance of the Fibrinogen proteins at 280 nm[25] was analyzed on a HP 8453 UV-Vis spectrophotometer equipped with a Peltier cell using a quartz cuvette (1 cm path length). Each coating was measured in triplicate. The absorbance values obtained were interpolated in the corresponding Fibrinogen calibration curves, built from PBS protein solutions of 0.1 to 1 $mg{\cdot}ml^{-1}$ and having a good linearity in the measured concentration range with an R^2 of 0.9999. (Calibration curved provided in the Supporting Information, Figure S3).

2.2 Trimethylene carbonate (TMC) monomer and polycarbonate polymer (PC) synthesis

The monomer (TMC) and polymer (PC) were synthesized by applying the optimized conditions previously described by us.[26] TMC synthesis: Ethyl chloroformate (25 mL, 0.262 mol) was added to a solution of 1,3-propanediol (10 g, 0.132 mol) dissolved in 500 mL of tetrahydrofuran (THF), in a dry nitrogen atmosphere. The reaction mixture was cooled with an ice bath and TEA was added dropwise over a period of 30 minutes. After 2 hours the white precipitate formed, triethylamine hydrochloride, was filtered off through a neutral aluminum oxide column. The filtered solution was then concentrated in a rotavapor and a white solid was precipitated in 200 mL of diethyl ether and left overnight in the fridge. The white precipitate (TMC) was collected by filtration and washed with diethyl ether (3 × 20 mL). TMC was dried overnight under vacuum at 35 °C before use. Yield: 54%. ^{1}H-NMR ($CDCl_3$, 400 MHz, δ in ppm): 2.14 (m, 2H), 4.45 (t, 4H). ^{13}C-NMR ($CDCl_3$, 125 MHz, δ in ppm): 21.3, 67.9, 148.5. ATR FT-IR (ν in cm^{-1}): 2 954.9 (C-H st), 1 728.2 (C=O st), 1 188.1 (C-O st as).

PC synthesis: TMC (5.2 g, 51 mmol) and TMP (324 mg, 2.4 mmol) where added to a flask with 56 mL of dry toluene (monomer concentration 0.9 M). The mixture was immersed in an oil bath at 35 °C and left under dry nitrogen flow for 15 minutes. After this time TFA (184 µl, 2.4 mmol) was added. Then three vacuum-dry nitrogen cycles were applied to the mixture to ensure oxygen and water free conditions. The reaction mixture was stirred for 48 hours and thereafter 0.6 mL of pyridine were added to neutralize the acid and stop the reaction. The toluene fraction was evaporated in the rotavapor and the resulting oil was dissolved in 15 mL of DCM. The reaction mixture dissolved in

DCM was precipitated in 500 mL of diethyl ether and the polymer was obtained after decantation of the solvent and washing with diethyl ether (2 × 60 mL) as a colorless and sticky oil. Yield: 91%. PC characterization: ^{1}H-NMR ($CDCl_3$, 400 MHz, δ in ppm): 0.91 (t), 1.53 (m), 1.92 (m), 2.05 (m), 3.74 (t), 4.11 (s), 4.30-4.24 (m). ^{13}C-NMR ($CDCl_3$, 125 MHz, δ in ppm): 7.25, 21.88, 28.03, 31.63, 42.69, 58.86, 64.30, 64.48, 65.03, 154.79, 154.90, 155.26. ATR FT-IR (ν in cm^{-1}): 3 554.8 (OH), 2 970.4 (C-H st), 1 735.9 (C=O st), 1 226.7 (C-O st as). GPC M_n 2826 g·mol^{-1}, $Đ$ = 1.19. MALDI maximums (m/z): 1339 (linear, number of TMC repeating units, n=12)) and 1805 (tri-branched, 3n=16) g/mol. Polymer mixture molar composition: ~34% linear, ~66% tri-branched. Polymer mixture hydroxyl group functionality per mol: 2.7. T_g = –36 °C.

2.3 Coating preparation

Coating solutions were prepared from stock solutions of PC (25 wt.%), crosslinker tHDI (50 wt.%) and mPEG550 (or mPEG1000, or mPEG2000) (25 wt.%) in dry cyclohexanone. mPEG1000 and mPEG2000 stock solutions were heated at 50 °C for several minutes until complete dissolution was achieved. Stock solutions were mixed at NCO:OH functional group mol ratio of 1.1 and PCL:mPEG functional group mol ratio of 9, reaching a final coating solution solid content of 27-28 wt.%. As a control sample (reference coating) a coating was prepared without mPEG chains, containing only PC and tHDI. The stock solution and final coating solution were prepared under argon atmosphere. The glass substrates (dimensions 20 x 75 mm or 20 x 20 mm) were rinsed with acetone, ethanol, dried overnight at 100 °C and finally treated for 15 minutes with UV/ozone (Novascan PSD-UVT). The coatings solutions were applied with a doctor blade squared applicator with a 120 μm spacing on the previously cleaned substrates. The coatings were cured by a using first applying 125 °C for 2 hours and a second, overnight curing/drying step at 60 °C, both in dry nitrogen atmosphere. The typical thickness of the coatings obtained after curing was between 7-10 μm.

The coatings were also prepared as free standing films by using aluminum cups (with ≈ 6 cm diameter). Approximately 0.8-1 grams of coating solution were poured into the cups and cured in the same way as described previously. The typical thicknesses for free standing films were ≈ 40 μm.

3. Results and discussion

3.1 Polycarbonate (PC) polymers synthesis

Due to their interesting thermal and mechanical properties, aliphatic PCs find applications in a wide variety of fields such as in regenerative medicine, drug delivery and in the coatings industry.[27-30] Furthermore, PCs typically present longer hydrolytic stability in water than comparable polyesters, are highly transparent to visible light and have a tunable and generally low T_g value.[31-33] Although this low Tg can be envisaged as a major drawback for some applications, they are advantageous for preparing protective and functional coatings which are required to interact favorably with water. This type of polymers can confer long-time water stability and high transparency to the coatings while immersed in water, and also the proper mobility in the system for self-replenishing. Additionally, PCs can be prepared by Cationic Ring Opening Polymerization (CROP) via green approaches using organic acids (*e.g.* TFA) as catalysts, resulting in metal-free polymers.

The PC polymeric matrix used in this work was synthesized with optimized polymerization conditions as described in our previous work.[26] Briefly, trimethylene carbonate (TMC) was used as monomer and a trifunctional alcohol, trimethylolpropane (TMP), was used as initiator, obtaining a polymer mixture composed of a ≈ 66% of tri-branched and ≈ 34% of linear polycarbonate (the PC polymer mixture chemical structures are represented in Figure 1). This polymer mixture was always obtained due to the coexistence of two polymerization mechanisms, the Activated Chain End (ACE) and Activated Monomer (AM) mechanism. A complete characterization by NMR, GPC and MALDI was crucial to discriminate the polymer composition and characteristics, as the difference between the two types of polymers is only detectable by MALDI (full polymer synthesis and characterization details are given in the materials and method section).

Peer-reviewed version available at Coatings 2018, 8, 184; doi:10.3390/coatings8050184

This approach allowed the preparation of metal-free polymers, with low *Đ* value, well-known chemical structure and composition and very high stability in aqueous conditions, as will be demonstrated. These are valuable characteristics when biomedical, pharmaceutical or non-toxic materials for green technologies are targeted.

3.2 Coatings preparation and characterization: surface wettability and stability

The coatings solutions were prepared by combining stock solutions of the synthesized PC polymers with the different molecular weight mPEG hydrophilic dangling chains, mPEG550, mPEG1000 or mPEG2000, and the crosslinker tHDI, from now on referred as PC-mPEGy, being "y" the mPEG molecular weight, *i.e.* 550, 1000 or 2000 g·mol^{-1}. A reference coating composed by PC and tHDI was also made in order to study the effect of mPEG chains in the polycarbonate coatings properties (named as PC-reference). The variation of mPEG with different molecular weight was done to investigate the influence of the dangling chain length in the coating features: hydrophilicity, anti-fouling properties and self-replenishing behavior.

Crosslinking of the coatings was done with thermal curing via the reaction between the tHDI isocyanate groups and the hydroxyl groups present in both the PC polymer precursors and the mPEG dangling chains, producing a polyurethane network (Figure 1a).

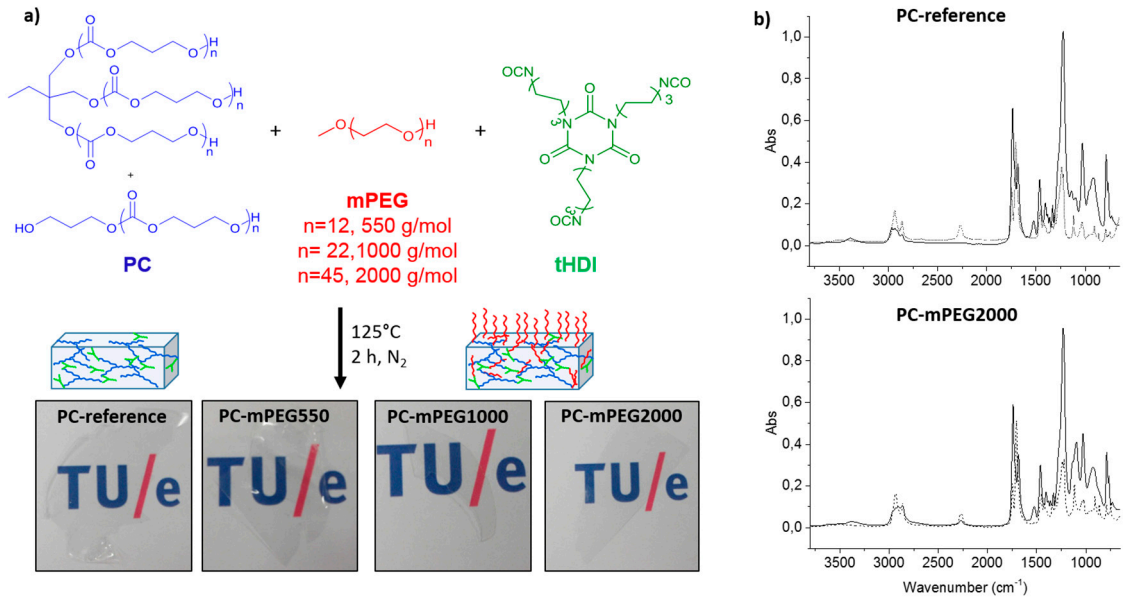

Figure 1. a) Chemical structure of the coating components and coating preparation. The images show transparent and colorless free standing coating films after curing (the transparent pieces were placed over a white paper with a logo for easier visualization). b) (top) FTIR of PC-reference and (bottom) PC-mPEG2000: (dashed lines) – coating solutions before curing; (solid lines) – solid film after curing.

The chemical crosslinking of the coatings was analyzed with FTIR by measuring the initial coating solution before curing and the obtained film after curing. PC-reference and PC-mPEG2000 FTIR spectra are shown in Figure 1b as representative examples. After the curing reaction the characteristic vibration bands of the isocyanate (υNCO ≈ 2300 cm^{-1}) and hydroxyl groups (υOH ≈ 3500 cm^{-1}) were no longer present and the new vibration bands assigned to the urethane bonds formation at (δNH ≈ 1500 cm^{-1} and υNH ≈ 3400 cm^{-1}) were detected. It is worth noting that for some coatings, *e.g.* PC-mPEG2000 (Figure 1b, bottom), a residual isocyanate peak remains after curing. This can be due to the slight excess of tHDI crosslinker added in the coating formulation (NCO:OH functional group mol ratio of 1.1) and the higher viscosity of mPEG2000, which has also a slight influence on the amount of extractable residues obtained in these coatings, as discussed below. Nevertheless, all

the synthesized PC coatings were free of application defects, colorless and highly transparent after curing, as can be observed in Figure 1a.

To investigate further the incorporation of the different components in the cross-linked network, extraction experiments were performed in water and acetone to determine the coatings mass loss (Table 1). The coatings mass loss after curing is attributed to non-reacted or non-network incorporated components which dissolve into the extraction solvents. For both, acetone and water extraction, the coatings remained visually unchanged after the immersion time. When comparing the water and acetone weight loss values, a lower weight loss was observed in water for all the coatings, which was expected due to the better solubility of all the coating components in acetone. This was confirmed by the ^{1}H-NMR analyses performed on the dried solid residues (Figure S1, supporting information). In the residues from the acetone extract, traces of all the coating components, PC, mPEG dangling chains and tHDI crosslinker, were detected. For the residues of the water extracts, mPEG and tHDI were mostly found, since the PC polymer is nearly insoluble in water. Overall, the low amount of weight loss detected, reaching a maximum of 6 % in acetone for PC-mPEG2000, confirms that covalently bonded coating networks were efficiently formed and are rather stable in the tested solvents.

The highest weight loss registered for PC-mPEG2000 coatings in both solvents can be related to an incomplete reaction of the isocyanate groups due to a lower availability of the hydroxyl groups, in view of the higher molecular weight of PEG2000, its higher viscosity and lower solubility which ultimately affects more strongly the chain mobility and its incorporation to the network. This observation is also corroborated by the remaining isocyanate peak observed in the FTIR spectrum after curing (Figure 1b), as discussed above.

Table 1. PC coatings characterization: Weight loss after immersion in water or acetone, water uptake, static contact angle in water soaked coatings, Glass Transition Temperature (T_g) values and protein (Fibrinogen) adhesion tests.

	Weight loss (%)		**Water Uptake (%)**	**Static Contact Angle (°)**	**T_g (°C)**	**Fibrinogen adhesion (μg·cm^{-2})**
	Water	Acetone				
PC-Reference	0.65 ± 0.4	1.7 ± 0.1	2.4 ± 0.7	79 ± 1.5	-10	11.2 ± 0.4
PC-mPEG550	0.67 ± 0.5	3.4 ± 0.05	4.5 ± 0.4	69.9 ± 1.1	-12	5.8 ± 0.3
PC-mPEG1000	0.68 ± 0.2	4.5 ± 0.8	12.1 ± 1.6	66 ± 1	-14	10.1 ± 1
PC-mPEG2000	3 ± 0.1	6.3 ± 0.2	26.2 ± 1.5	51 ± 0.75	-34	12.8± 0.5

After confirming proper network formation, the influence of the dangling chains on the coatings properties, *i.e.* water uptake, wettability and T_g, was analyzed (Table 1). The incorporation of the PEG-based hydrophilic dangling chains allowed tuning of the coatings hydrophilicity. The hydrophilicity of the coatings increased with the length of the dangling chains, as denoted by the ability of absorbing more water and the lower static water contacts angles obtained. This is in accordance with the expectation that the introduction of more hydrophilic ethylene oxide units in the network via the dangling chains will allow more water-polymer interactions via hydrogen bonding. As for the thermal properties of the coatings, a decrease in T_g was observed when introducing mPEG, this decrease being more pronounced for the longer dangling chains.

In the search for materials with long-time durability, the stability and appearance of the coating along with the surface wettability in time are important parameters. The stability of the coatings was estimated by measuring the water uptake in time. The cleavage of the urethane and carbonate bonds could lead to a more hydrophilic network and probably loss of the network structural integrity, meaning that a higher capacity of absorbing water and thus an increase in the water uptake value should be observed in time. On the other hand, the release of small coating fragments of coating into the solvent could also lead to a decrease in water uptake. As for the surface wettability, a decrease of the water contact angle would indicate the formation of more hydrophilic groups on the surface, most

likely due to degradation as explained before. On the contrary, an increase in contact angle would indicate a loss of the hydrophilicity due to the loss of the hydrophilic dangling chains at the surface.

In spite of all these possible scenarios, the water uptake and contact angle of the PC coatings prepared remained remarkably constant over one year of immersion in water, as can be seen in Figure 2, demonstrating the excellent stability of the coatings. Interestingly the coatings appearance was also the same as the initial coatings, keeping their integrity, transparency and not developing any color in time, which is a further indication of absent degradation (Figure S2). The excellent stability of the coatings was further confirmed by the low weight loss of the coatings after one year immersion in water, reaching a maximum of only ≈ 3.1 % loss (Figure S2).

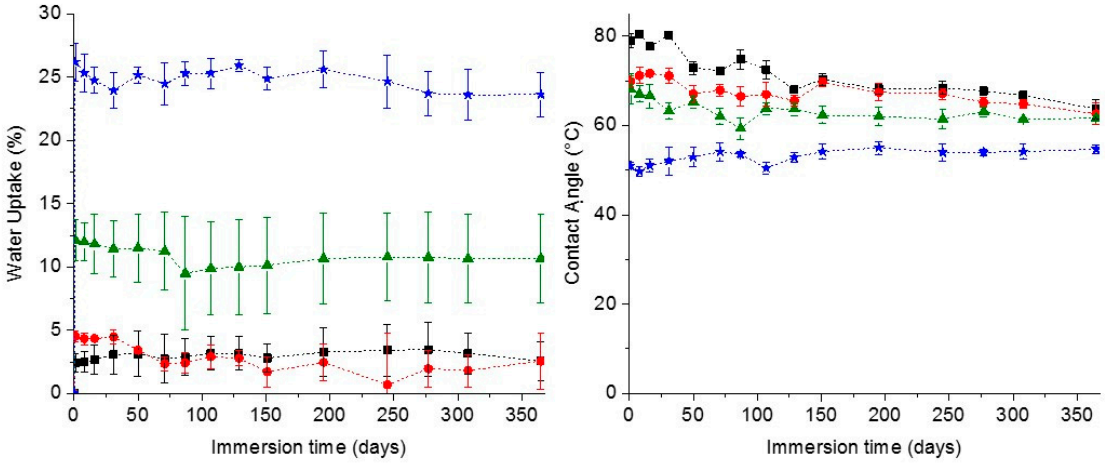

Figure 2. Coatings stability during one year of immersion in water: Water uptake (%), left and static contact angle, right. Squares – PC-reference, circles – PC-mPEG550, triangles – PC-mPEG1000 and stars PC-mPEG2000 coatings.

3.3 Evaluation of anti-fouling properties

Biofouling is a complex process that involves several stages.[34] In the first minutes after immersion of a material in water proteins adsorb on the surfaces forming a conditioning film which establishes the proper environment (biofilm or slime) for the attachment of bigger organisms during the next stages, micro- and macro-fouling. The fouling problem is even more complex due to the fact that it is also influenced by external factors, like water salinity, oxygen concentration, temperature and light-exposure period, which vary across the globe and for the type of water .[1] A simplified, laboratory accessible way to evaluate the anti-fouling properties is to quantify the first stage of biofouling by measuring the protein adsorption on surfaces. Thus surfaces presenting a low protein adsorption value can be considered to be of high potential for anti-fouling since the prevention of primary phase of fouling (biofilm formation) ensures the impossibility of bigger organisms to adsorb and settle afterwards.

In this study Fibrinogen (FB) was selected as model protein-foulant to evaluate the fouling potential of the PC coatings prepared. The quantification of the adsorbed FB was done by UV/Vis spectroscopy and making use of the characteristic absorption peak of these proteins at 280 nm, due to the presence of aromatic aminoacids in their chemical structure.[24-25] The coatings were fully covered with a known amount of a PBS solution of FB. The adsorbed proteins were quantified by determining the proteins remaining in the PBS solution (not-absorbed) after 24 hours of incubation and with reference to a previously prepared calibration curve (see Figure S3 in Supporting Information).

The FB adsorption value was determined to be very close to 10 $\mu g \cdot cm^{-2}$ for all the coatings prepared which is normally considered as a low protein adsorption value in the related AF literature (Table 1). [23] Such low protein adsorption values denote the very good stability of these coatings and their high potential for AF. In fact, the protein adsorption determination procedure was

Peer-reviewed version available at Coatings 2018, 8, 184; doi:10.3390/coatings8050184

sometimes rather difficult and inconclusive due to the very low values measured. For this purpose the coatings were always measured in triplicate and with extra care to avoid contamination or any loss of material from the PBS solutions.

As can be seen from Table 1, the introduction of the shortest mPEG hydrophilic dangling chains, mPEG550, resulted in the maximum decrease of protein adsorption value as compared to the reference. However, when increasing the coating hydrophilicity further, *i.e.* introducing the mPEG1000 or mPEG2000 chains, the protein adhesion values did not decrease further, with the protein adsorption value for these coatings very close to the value of the PC-reference coating. Hence, no clear correlation was found between the reference coatings and the increasing hydrophilicity via the introduction of mPEG dangling chains with different length. The presence of a mPEG molecular weight threshold value for which a minimum of protein adsorption value is found was also reported by others when using FB or other proteins like Bovine Serum Albumin(BSA).[35-36]

Although protein-PEG interactions have been widely studied, they are still far from being understood, and up to date there is not a clear explanation for this. A possible explanation which has been put forward for the lower efficiency of high molecular weight PEG relates either to the difficulty in achieving an optimum chain density at the surface due to possible entanglements (which is crucial for achieving a minimum protein adsorption value), or to the reduced mobility of the longer PEG chains. [36-37] Another possible explanation relies on the solubility of PEG in aqueous solutions with high salt concentrations, with particularly sensitivity to sodium and potassium phosphate salts, which are in fact present in the PBS solution used for the FB experiments.[38-39] Hence, our results showing inefficient protein adsorption reduction when using high molecular weight mPEG chains can be due to the reduced solubility of the mPEG in the PBS solution that hinders the water-polymer hydrogen bonding interactions and favors protein adsorption. Since we cannot determine in this work the accurate surface coverage of the coatings by the dangling chains, we can also not discard, however, the possibility of entanglements causing a lower chain density for the longest mPEG chains.

3.4 Self-replenishing behavior: surface hydrophilicity recovery after damage

To study the self-replenishing of the surface functionalities that guarantee the extended life-time of the hydrophilicity and the long-term use of the coatings, a controlled damage was introduced by a set-up previously used for analogous self-replenishing coatings, as described elsewhere.[18] Briefly, coatings were damaged with sand paper by applying a constant force and moving a specific weight back and forth on top of the coating for a specific number for 150 cycles. Afterwards the coatings were re-immersed in water at room temperature and at different recovery times, up to 22 hours (Figure 3).

The thickness of the coatings was re-measured after the damage confirming the removal of a few micrometers of the most external top coating layers. The decrease in thickness was ≈ 0.5 μm for the PC-reference coating and ranging from 1.3 to 1.5 μm for the softer mPEG containing coatings. The extent of recovery, concerning the initial loss of hydrophilicity, was evaluated by comparing the initial dynamic water contact angle (CA_{Adv}) of the water-soaked coatings before (Figure 3a) and after damage, at different times of recovery in water, *e.g.* 1, 2, 4 and 22 hours (Figure 3b) and quantified by calculating the Self-Replenishing Efficiency (SRE Figure 3c).

The damage experiments were first done on dry and also wet conditions (*i.e.* coatings immersed in water), however, only the results from the "dry-damage" could be used reliably since during the "wet-damage" the coatings were often detached from the substrate hampering the analyses afterwards. Note that in real systems, a primer would probably be required to ensure the adhesion of the hydrophilic coatings to different substrates.

After the "dry damage" the coatings were immediately immersed in water to re-expose the newly created surfaces to water for the replenishing to take place. One of the limitations of this procedure is that after the damage and re-immersion in water, the coatings need to absorb water and swell, hence, it was not possible to estimate the extent of damage immediately after it takes place, and a reliable measurement of the water CA_{Adv} could only be done after 1 hour of immersion (Figure 3). This was the time needed for the coatings to reach a maximum swelling ratio, as estimated from

Preprints (www.preprints.org) | NOT PEER-REVIEWED | Posted: 15 March 2018 doi:10.20944/preprints201803.0114.v1

Peer-reviewed version available at Coatings 2018, 8, 184; doi:10.3390/coatings8050184

the swelling ratio (W_t/W_0) profiles (Figure S4, supporting information) and to minimize the effect of the water absorption on CA measurements.

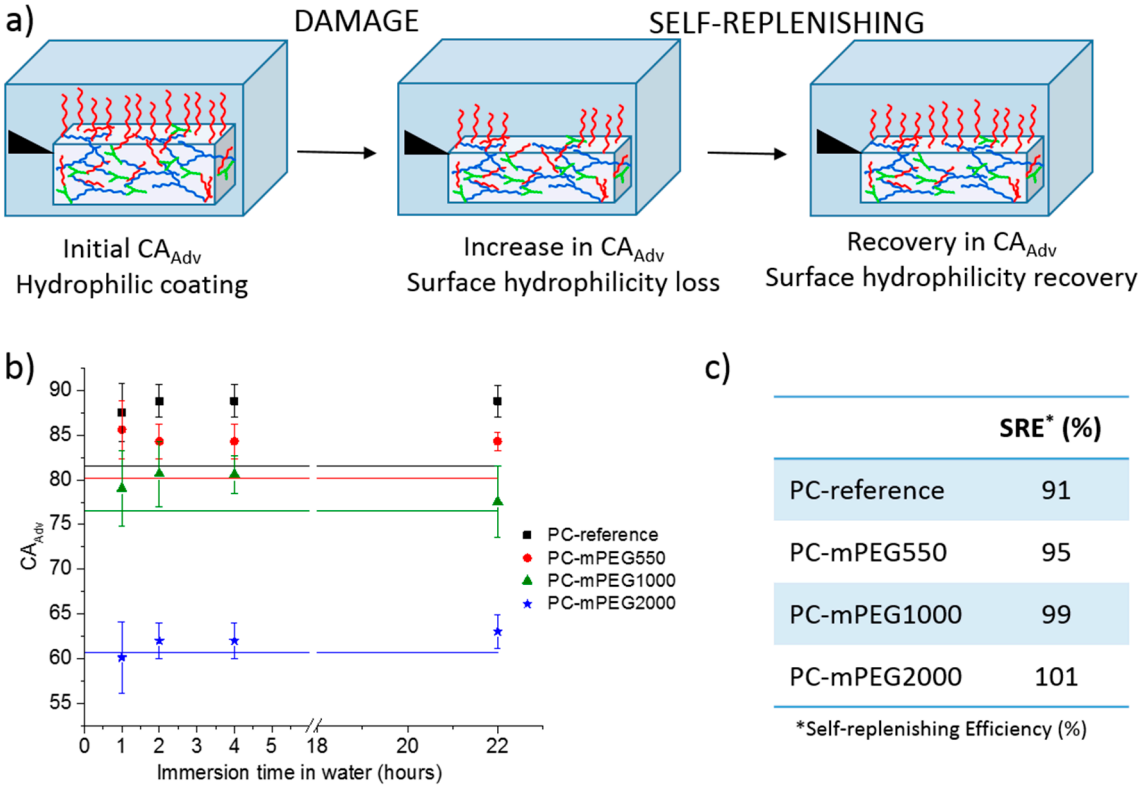

Figure 3. a) Schematic of the surface damage and recovery of the water-soaked coatings. b) Advancing water contact angle (CA_{Adv}) of the coatings after damage, at different times of recovery upon immersion in water. Solid lines represent the initial water CA_{Adv} before damage. Black squares and line – PC-ref, red circles and line – PC-mPEG550, green triangles and line – PC-mPEG1000 and blue stars and line – PC-mPEG2000 coatings. c) Self-replenishing Efficiency (%).

An initial increase in the water CA_{Adv} after damage, *i.e.* loss of hydrophilicity, as compared to the initial water CA_{Adv} of the non-damaged coatings (solid straight lines in Figure 3b), was observed for all coatings except for the PC-mPEG2000 (Figure 3b).

For the PC-reference coating an increase in CA_{Adv} was detected after damage and 1 hour of recovery in water. This increase in hydrophobicity can be explained by the fact that the damage imposed removes a few micrometers of the initial coatings surface, which may be slightly more hydrophilic than the bulk, as it may contain residual unreacted hydroxyl groups or more hydrophilic segments. Hence, when the bulk of the coatings is exposed by the damage, more hydrophobic segments will be at the new created surfaces increasing the newly measured water CA_{Adv}. Upon re-immersion in water, the PC-reference coating is not able to recover the initial hydrophilicity, not even after 22 hours of immersion. This was expected since this coating does not contain additional hydrophilic dangling chains in the bulk, and the surface initially formed during the curing process with eventually more hydrophilic segments was lost during the damage, *i.e.* the PC-reference has no reservoir of hydrophilic components, Figure 3b (black squares).

For the mPEG-containing coatings a different replenishing behavior was found depending on the type of PEG used. For PC-mPEG550 and PC-mPEG1000 after damage and one hour recovery, a significant increase in CA_{Adv} was detected (Figure 3b). After 22 hours of immersion in water, the PC-mPEG550 presented a partial or null CA_{Adv} recovery in water, but the PC-mPEG1000 was able to recover the initial CA_{Adv}. The ability to recover the surface composition results from the combination of a low T_g, that ensures the proper mobility of the dangling chains towards the water-coating interface, and the dangling chain length which also endows these mobility and interface

reorientation.[40] These coatings present similar T_g values (Table 1) thus showing that the mPEG dangling chain length plays a major role on the self-replenishing ability, *i.e.* only for PC-mPEG1000 the surface hydrophilicity was fully recovered, as demonstrated by the calculated SRE (Figure 3c)

For PC-mPEG2000 coatings no significant change of the water CA_{Adv} was observed after the damage or any of the recovery times (Figure 3b). In this case, the combination of a much lower T_g (Table 1) and longer dangling chains seems to provide very stable hydrophilic coatings which can recover their hydrophilicity on damaged surfaces really fast (at least on a time-scale shorter than 1 hour, hence, not possible to detect with our procedure) upon immersion on water at room temperature. In fact, the excellent stability shown for all the PC coatings (Figure 2), and in particular for the PC-mPEG1000 and PC-mPEG2000, already hinted that the surface composition of these coatings is very stable and/or replenishes in time, as the water CA remained constant throughout one year.

4. Conclusions

PC polymers were successfully used in the preparation of cross-linked hydrophilic coatings which are colorless and transparent, with very low leachable amounts. The coatings present tunable hydrophilicity depending on the type (molecular weight) of mPEG dangling chains added to the cross-linked network, as well as, an excellent long-term stability in water, as shown by the unchanged visual appearance and constant surface hydrophilicity after one year of immersion in water.

The proper selection of the coatings components confers an intrinsic self-replenishing driving force due to the hydrophobic/hydrophilic balance between the bulk and surface-oriented components. Once the hydrophilicity was reduced upon surface damage, the hydrophilic dangling chains in the bulk (*i.e.* in the reservoir) are exposed at the new wet and damaged surfaces and their reorientation towards the water coating interface takes place, minimizing the exposure of the more hydrophobic segments of the PC coatings. The combination of a low T_g and sufficient mPEG dangling chain length ensured the system mobility and the nearly 100% recovery of the surface hydrophilicity for the PC-mPEG1000 and PC-mPEG2000 coatings. Furthermore, these coatings showed an excellent stability in water throughout a one year evaluation period which may be due to the efficient preparation of cross-linked networks in which all the components (including the hydrophilic dangling chains) are covalently bonded, as well as, to the self-replenishing processes taking place during the period that the coatings are immersed in water.

Finally, all the coatings exhibit low protein (Fibrinogen) adhesion on their surfaces, reaching a real minimum of protein adsorption for the PC-mPEG550, which demonstrates the high potential of application of these coatings as anti-fouling and self-replenishing protective films.

Supplementary Materials: The following material is available online at www.mdpi.com/link, Figure S1: ^{1}H-NMR spectra (400 MHz, $CDCl_3$) for PC-mPEG2000 acetone and water extracts, and pure coatings components, tHDI, mPEG2000 and PC polymer, Figure S2: Coatings appearance and weight loss (%) after 1 year water immersion. PC and PC-mPEG2000 images after 1 year immersion in water. Transparent and colorless free standing coatings placed on top of a logo. Figure S3: Calibration curve for the Fibrinogen absorption experiments. Figure S4. Swelling ratio profiles (weight of water swollen coating at different immersion times (W_t) divided by the initial dried coating (W_0)) for coatings immersed in water for 24 hours.

Acknowledgments: The authors thank the Netherlands Enterprise Agency (RVO) for funding via the IOP Self-Healing Materials program in the Netherlands (project # SHM012044). Mr H. Scholten, Ms P. Mommers and Ms L.M. Struik are acknowledged for small experimental or characterization contributions during their graduation projects.

Author Contributions: I. Jimenéz-Pardo and A.C.C. Esteves conceived and designed the experiments; I. Jimenéz-Pardo performed the experiments; L.G.J. van der Ven, R.A.T.M. van Benthem, G. de With and A.C.C. Esteves contributed with regular discussions during the analyzes of the data; I. Jimenez-Pardo wrote the paper.

Conflicts of Interest: "The authors declare no conflict of interest."

References

(1) Yebra, D. M.; Kiil, S.; Dam-Johansen, K. Antifouling technology—past, present and future steps towards efficient and environmentally friendly antifouling coatings. *Progress in Organic Coatings* **2004**, *50*, 75-104.

(2) Schultz, M. P.; Bendick, J. A.; Holm, E. R.; Hertel, W. M. Economic impact of biofouling on a naval surface ship. *Biofouling* **2011**, *27*, 87-98.

(3) Campoccia, D.; Montanaro, L.; Arciola, C. R. A review of the biomaterials technologies for infection-resistant surfaces. *Biomaterials* **2013**, *34*, 8533-8554.

(4) Dellimore, K. H.; Helyer, A. R.; Franklin, S. E. A scoping review of important urinary catheter induced complications. *Journal of Materials Science: Materials in Medicine* **2013**, *24*, 1825-1835.

(5) Nurioglu, A. G.; Esteves, A. C. C.; de With, G. Non-toxic, non-biocide-release antifouling coatings based on molecular structure design for marine applications. *Journal of Materials Chemistry B* **2015**, *3*, 6547-6570.

(6) Banerjee, I.; Pangule, R. C.; Kane, R. S. Antifouling coatings: Recent developments in the design of surfaces that prevent fouling by proteins, bacteria, and marine organisms. *Advanced Materials* **2011**, *23*, 690-718.

(7) Genzer, J.; Efimenko, K. Recent developments in superhydrophobic surfaces and their relevance to marine fouling: A review. *Biofouling* **2006**, *22*, 339-360.

(8) Krishnan, S.; Weinman, C. J.; Ober, C. K. Advances in polymers for anti-biofouling surfaces. *Journal of Materials Chemistry* **2008**, *18*, 3405-3413.

(9) Callow, J. A.; Callow, M. E. Trends in the development of environmentally friendly fouling-resistant marine coatings. *Nature Communications* **2011**, *2*, ISSN 2041-1723.

(10) Rufin, M. A.; Gruetzner, J. A.; Hurley, M. J.; Hawkins, M. L.; Raymond, E. S.; Raymond, J. E.; Grunlan, M. A. Enhancing the protein resistance of silicone via surface-restructuring peo-silane amphiphiles with variable peo length. *Journal of Materials Chemistry B* **2015**, *3*, 2816-2825.

(11) Yandi, W.; Mieszkin, S.; Martin-Tanchereau, P.; Callow, M. E.; Callow, J. A.; Tyson, L.; Liedberg, B.; Ederth, T. Hydration and chain entanglement determines the optimum thickness of poly(hema-co-peg(10)ma) brushes for effective resistance to settlement and adhesion of marine fouling organisms. *ACS Applied Materials & Interfaces* **2014**, *6*, 11448-11458.

(12) Ju, H.; McCloskey, B. D.; Sagle, A. C.; Kusuma, V. A.; Freeman, B. D. Preparation and characterization of crosslinked poly(ethylene glycol) diacrylate hydrogels as fouling-resistant membrane coating materials. *Journal of Membrane Science* **2009**, *330*, 180-188.

(13) Gu, Y.; Zhou, S.; Luo, H.; Wu, L.; Gao, W.; Yang, J. Temperature-dependent phase-segregation behavior and antifouling performance of uv-curable methacrylated pdms/peg coatings. *Journal of Polymer Science Part B: Polymer Physics* **2016**, *54*, 1612-1623.

(14) Gudipati, C. S.; Finlay, J. A.; Callow, J. A.; Callow, M. E.; Wooley, K. L. The antifouling and fouling-release perfomance of hyperbranched fluoropolymer (hbfp)-

poly(ethylene glycol) (peg) composite coatings evaluated by adsorption of biomacromolecules and the green fouling alga ulva. *Langmuir* **2005**, *21*, 3044-3053.

(15) Jeon, S. I.; Lee, J. H.; Andrade, J. D.; De Gennes, P. G. Protein—surface interactions in the presence of polyethylene oxide: I. Simplified theory. *Journal of Colloid and Interface Science* **1991**, *142*, 149-158.

(16) Heuberger, M.; Drobek, T.; Spencer, N. D. Interaction forces and morphology of a protein-resistant poly(ethylene glycol) layer. *Biophysical Journal* **2005**, *88*, 495-504.

(17) Zhang, Y.; Rocco, C.; Karasu, F.; van der Ven, L. G. J.; van Benthem, R. A. T. M.; Allonas, X.; Croutxé-Barghorn, C.; Esteves, A. C. C.; de With, G. Uv-cured self-replenishing hydrophobic polymer films. *Polymer* **2015**, *69*, 384-393.

(18) Esteves, A. C. C.; Luo, Y.; van de Put, M. W. P.; Carcouët, C. C. M.; de With, G. Self-replenishing dual structured superhydrophobic coatings prepared by drop-casting of an all-in-one dispersion. *Advanced Functional Materials* **2014**, *24*, 986-992.

(19) Dikić, T.; Ming, W.; van Benthem, R. A. T. M.; Esteves, A. C. C.; de With, G. Self-replenishing surfaces. *Advanced Materials* **2012**, *24*, 3701-3704.

(20) Chen, K.; Wu, Y.; Zhou, S.; Wu, L. Recent development of durable and self-healing surfaces with special wettability. *Macromolecular Rapid Communications* **2016**, *37*, 463-485.

(21) Wang, Z. H.; van Andel, E.; Pujari, S. P.; Feng, H. H.; Dijksman, J. A.; Smulders, M. M. J.; Zuilhof, H. Water-repairable zwitterionic polymer coatings for anti-biofouling surfacese. *Journal of Materials Chemistry B* **2017**, *5*, 6728-6733.

(22) Kuroki, H.; Tokarev, I.; Nykypanchuk, D.; Zhulina, E.; Minko, S. Stimuli-responsive materials with self-healing antifouling surface via 3d polymer grafting. *Advanced Functional Materials* **2013**, *23*, 4593-4600.

(23) Chen, K.; Zhou, S.; Wu, L. Self-healing underwater superoleophobic and antibiofouling coatings based on the assembly of hierarchical microgel spheres. *ACS Nano* **2016**, *10*, 1386-1394.

(24) Aitken, A.; Learmonth, M. P. In *The protein protocols handbook*; Walker, J. M., Ed.; Humana Press: Totowa, NJ, 2009.

(25) Zhong, D.; Zhang, Y.; Zuo, Q.; Liu, Z.; Xue, W. Interaction of polyethyleneimines with fibrinogen and erythrocyte membrane. *Soft Materials* **2014**, *12*, 138-148.

(26) Jiménez-Pardo, I.; van der Ven, L. G. J.; van Benthem, R. A. T. M.; Esteves, A. C. C.; de With, G. Effect of a set of acids and polymerization conditions on the architecture of polycarbonates obtained via ring opening polymerization. *Journal of Polymer Science Part A: Polymer Chemistry* **2017**, *55*, 1502-1511.

(27) Feng, J.; Zhuo, R.-X.; Zhang, X.-Z. Construction of functional aliphatic polycarbonates for biomedical applications. *Progress in Polymer Science* **2012**, *37*, 211-236.

(28) Brannigan, R. P.; Dove, A. P. Synthesis, properties and biomedical applications of hydrolytically degradable materials based on aliphatic polyesters and polycarbonates. *Biomaterials Science* **2017**, *5*, 9-21.

587 (29) Wang, H.; Wang, Y.; Chen, Y.; Jin, Q.; Ji, J. A biomimic ph-sensitive polymeric
588 prodrug based on polycarbonate for intracellular drug delivery. *Polymer Chemistry*
589 **2014**, *5*, 854-861.
590 (30) Voo, Z. X.; Khan, M.; Narayanan, K.; Seah, D.; Hedrick, J. L.; Yang, Y. Y.
591 Antimicrobial/antifouling polycarbonate coatings: Role of block copolymer
592 architecture. *Macromolecules* **2015**, *48*, 1055-1064.
593 (31) Suriano, F.; Coulembier, O.; Hedrick, J. L.; Dubois, P. Functionalized cyclic
594 carbonates: From synthesis and metal-free catalyzed ring-opening polymerization to
595 applications. *Polymer Chemistry* **2011**, *2*, 528-533.
596 (32) Xu, J.; Feng, E.; Song, J. Renaissance of aliphatic polycarbonates: New techniques
597 and biomedical applications. *Journal of Applied Polymer Science* **2014**, *131*, ISSN
598 0021-8995.
599 (33) Wang, X.-L.; Zhuo, R.-X.; Liu, L.-J.; He, F.; Liu, G. Synthesis and characterization
600 of novel aliphatic polycarbonates. *Journal of Polymer Science Part A: Polymer*
601 *Chemistry* **2002**, *40*, 70-75.
602 (34) Graham, M.; Cady, N. Nano and microscale topographies for the prevention of
603 bacterial surface fouling. *Coatings* **2014**, *4*, 37-59.
604 (35) Gudipati, C. S.; Finlay, J. A.; Callow, J. A.; Callow, M. E.; Wooley, K. L. The
605 antifouling and fouling-release perfomance of hyperbranched fluoropolymer
606 (hbfp)−poly(ethylene glycol) (peg) composite coatings evaluated by adsorption of
607 biomacromolecules and the green fouling alga ulva. *Langmuir* **2005**, *21*, 3044-3053.
608 (36) Benhabbour, S. R.; Sheardown, H.; Adronov, A. Protein resistance of peg-
609 functionalized dendronized surfaces: Effect of peg molecular weight and dendron
610 generation. *Macromolecules* **2008**, *41*, 4817-4823.
611 (37) Unsworth, L. D.; Sheardown, H.; Brash, J. L. Polyethylene oxide surfaces of variable
612 chain density by chemisorption of peo-thiol on gold: Adsorption of proteins from
613 plasma studied by radiolabelling and immunoblotting. *Biomaterials* **2005**, *26*, 5927-
614 5933.
615 (38) Taylor, W.; Jones, R. A. L. Protein adsorption on well-characterized polyethylene
616 oxide brushes on gold: Dependence on molecular weight and grafting density.
617 *Langmuir* **2013**, *29*, 6116-6122.
618 (39) Heeb, R.; Lee, S.; Venkataraman, N. V.; Spencer, N. D. Influence of salt on the
619 aqueous lubrication properties of end-grafted, ethylene glycol-based self-assembled
620 monolayers. *ACS Applied Materials & Interfaces* **2009**, *1*, 1105-1112.
621 (40) Esteves, A. C. C.; Lyakhova, K.; van Riel, J. M.; van der Ven, L. G. J.; van Benthem,
622 R. A. T. M.; de With, G. Self-replenishing ability of cross-linked low surface energy
623 polymer films investigated by a complementary experimental-simulation approach.
624 *The Journal of Chemical Physics* **2014**, *140*, 124902.
625

626